Desalination and Water Treatment
www.deswater.com
doi: 10.1080/19443994.2014.923332

55 (2015) 1229–1239
July

Taylor & Francis
Taylor & Francis Group

A ion-imprinted chitosan/Al_2O_3 composite material for selective separation of copper(II)

Jianxian Zeng[a,*], Huajun Chen[a], Xinke Yuan[b], Qiannan Guo[a], Xie Yu[a]

[a]*Key Laboratory of Theoretical Chemistry and Molecular Simulation of Ministry of Education, School of Chemistry and Chemical Engineering, Hunan Province College Key Laboratory of QSAR/QSPR, Hunan University of Science and Technology, Xiangtan 411201, China, Tel. +86 731 58290045; Fax: +86 731 58290509; emails: zengjianxian@163.com (J. Zeng), chj-youxiang@qq.com (H. Chen), guoqiannan66@126.com (Q. Guo), 125168967@qq.com (X. Yu)*
[b]*Technology Center of China Tobacco Hunan Industrial Co., Ltd., Changsha 410007, P.R. China, Tel. +86 015907367824; email: 215191627@qq.com*

Received 7 September 2013; Accepted 5 May 2014

ABSTRACT

A novel copper(II) ion-imprinted chitosan/aluminum oxide (IIP/Al_2O_3) has been prepared with the surface-grafted and surface imprinting technologies for selective adsorption of Cu (II) from aqueous solutions. Al_2O_3 powder, modified with tetraethyl orthosilicate, was used as the carrier material. Chitosan was employed as the functional monomer. The prepared IIP/Al_2O_3 was characterized by using the infrared spectra, scanning electron microscopy, and energy dispersive X-ray spectroscopy. Effects of pH and initial concentration of Cu(II) on the adsorption capacity of IIP/Al_2O_3 were investigated, and the adsorption kinetics and thermodynamics were also studied. Results showed that, the kinetic data were fitted well by the pseudo-second-order model. The adsorption equilibrium data were fitted well by the Langmuir isotherm model. The thermodynamic parameters indicated that the adsorption of Cu(II) on IIP/Al_2O_3 was an endothermic and spontaneous process. Further, the selectivity experiment was done for the mixed solutions containing Cu(II), Ni(II), and Zn(II). The selectivity factors of Cu(II) on IIP/Al_2O_3 were much higher than those of Ni(II) and Zn(II). After Cu(II) adsorption-desorption cycles were repeated 10 times by using the same IIP/Al_2O_3, the adsorption capacity of IIP/Al_2O_3 was decreased only 2%. The IIP/Al_2O_3 showed good stability and reusable properties.

Keywords: Surface ion-imprinted; Adsorption; Copper(II); Aluminum oxide; Selective separation

1. Introduction

Copper is essential to human life and health, but like all heavy metals it is potentially toxic especially at high concentrations [1]. Many wastewaters containing copper(II) come from industries like mining, non-ferrous metal industry, metalworking and finishing processes, electroplating, electrical and electronics, printing and photographic industries, and so on. Removal/recovery of Cu(II) is an important issue in the environmental and industrial fields [2–4]. Specifically, there is great interest in selective separation of individual Cu(II) in the aqueous phase. Chemical precipitation [5], complexation [6], solvent extraction [7], membrane separation [8], and ion

*Corresponding author.

exchange [9] have traditionally been the methods used to separate heavy metal ions; however, these methods have disadvantages, such as heterogeneous reactions and the need for additional reagents to complete the separation process [10].

Ion-imprinting is a powerful technique for preparing polymeric materials that are capable of high ionic recognition [11]. The ion-imprinting is a process in which the functional monomer and cross-linking agent copolymerize in the presence of template ions. After removing the template ions, the imprinted cavities providing tailor-made binding sites for the ions are left in the ion-imprinted polymer [12,13]. There are some reports on the applications of imprinted technique for separation and enrichment of heavy metal ions [14–18].

Surface imprinting is one of the important types of imprinting methods [19]. It in combination with the support process improves the kinetics of the adsorption and desorption by increasing the surface area, pore volume, and active binding sites of the adsorbents, and possesses high selectivity, good mass transfer, and fast binding rate. Moreover, the template ions can be removed easily from the ion-imprinted polymers [20]. Recently, some attempts have already been undertaken by means of the surface imprinting. Li et al. [21] tried to prepare ion-imprinted polymer in nano-TiO_2 matrix for selective separation of Pb(II). It has been reported by Shamsipur et al. [22] that selective adsorption of uranyl ion can be achieved by employing ion-imprinted polymers on the surface of silica gel particles. Li et al. [23] studied the preparation and recognition characteristic of surface ion-imprinting material IIP-PEI/SiO_2 of chromate anion. Pan et al. [12] also demonstrated that it was possible to separate strontium (II), selectively, by using an ion-imprinted polymer based on palygorskite as a sacrificial support. However, aluminum oxide (Al_2O_3) employed as a carrier material was seldom reported in the process of surface imprinting, and the surface-grafted technology was scarcely used to prepare the imprinting materials.

In this study, Al_2O_3 was used as a support in the surface imprinting technique because of its chemical, mechanical and thermal stability. In addition, Al_2O_3 is the main component of ceramic membrane. Base on the imprinting technique on Al_2O_3, we can graft easily ion-imprinted polymer onto the surface of Al_2O_3 ceramic membrane in another work. Copper(II), CTS, and glycidoxypropyltrimethoxysilane were used as the template ion, functional monomer, and cross-linking agent, respectively. A novel copper(II) ion-imprinted polymer/aluminum oxide (IIP/Al_2O_3) was prepared. Schematic illustration of the preparation of IIP/Al_2O_3 is shown in Fig. 1. The prepared IIP/Al_2O_3 was characterized by using the Fourier transform infrared spectroscopy (FT-IR), scanning electron microscopy (SEM), and energy dispersive X-ray (EDX). Then, the adsorption and desorption behaviors of Cu(II) on IIP/Al_2O_3 were described and discussed in detail.

2. Experimental

2.1. Apparatus

In some cases, the samples were examined under a JSM-6380LV SEM (JEOL, Japan) equipped with an Inca-350 EDX spectrometer (OXFORD, England). A Nicolet 6700 FT-IR (NICOLET, USA) was employed to record the infrared spectra by using KBr as background spectra. An AA-670 atomic absorption spectrophotometer (AAS) (SHIMADZU, Japan) was used for the determination of metal ions. A PE20 pH meter (METTLER TOLEDO, Switzerland) was employed to measure pH value.

2.2. Reagents and materials

Copper sulfate pentahydrate ($CuSO_4{\cdot}5H_2O$) as the Cu(II) template source, chitosan (CTS) with 95% deacetylation as the functional monomer, and glycidoxypropyltrimethoxysilane (KH-560) as the cross-linking agent were all purchased from Sinopharm Chemical Reagent Co. Ltd. (China). Tetraethyl orthosilicate (TEOS) as the silica source was purchased from Xilong Chemical Co., Ltd (China). Aluminum oxide powder as the support was received from Shanghai Wusi Chemical Reagent Co., Ltd (China). All other reagents were analytical reagent grade.

2.3. Deposition of SiO_2 active layer onto aluminum oxide powder

The SiO_2 active layer was prepared by the *in situ* hydrolysis deposit method. Firstly, aluminum oxide powder (2 g) was dipped into a hydrochloric acid solution of 0.6 mol L^{-1} for 15 h. The powder was washed with deionized water till neutral pH and dried in vacuum oven at 50 °C. Then, the dry powder was immersed into 1:10 (v/v) TEOS/ethanol and reacted at 70 °C for 30 h in a round-bottom flask equipped with a reflux condenser. After the reaction, the powder was washed in an ultrasonic bath for 10 min, and then calcined for 3 h at 600 °C to form a SiO_2 active deposit on the aluminum oxide powder. When cooled to room temperature, the powder was immersed in a hydrochloric acid solution of 0.1 mol L^{-1} for 24 h in order to activate the silanol groups. Then, the treated aluminum oxide powder

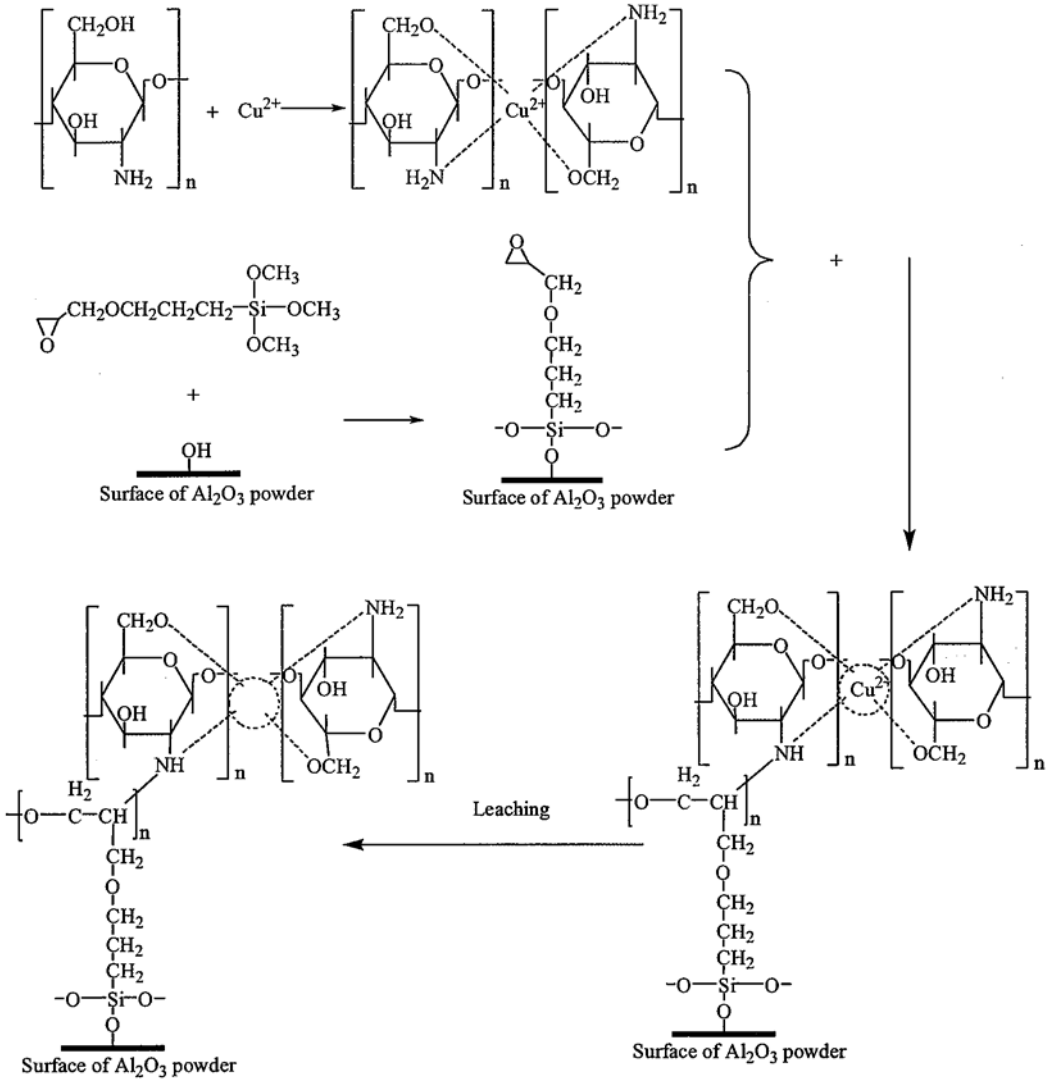

Fig. 1. Schematic illustration of the preparation of IIP/Al_2O_3.

was washed with deionized water till neutral pH and dried at 50℃.

2.4. Preparation of IIP/Al_2O_3

After the deposition of SiO_2 active layer, the powder was immersed into 1:5 (v/v) KH-560/acetone in a round-bottom flask equipped with a reflux condenser and stirred for 10 h at 70℃. CTS (3.0 g) and $CuSO_4{\cdot}5H_2O$ (0.25 g) were dissolved in 0.1 mol L^{-1} acetic acid aqueous solution of 150 mL and stirred for 2 h at 25℃. Then, the grafting reaction was initiated on the surface of the silanized powder at 35℃ for 5 h during continuous stirring. The prepared Cu-IIP/Al_2O_3 was dried at 35℃, then grinded and washed, respectively, with acetone and ethanol in order to remove the excessive KH-560. Further, the Cu-IIP/Al_2O_3 was washed with 1.0 mol L^{-1} hydrochloric acid solutions to remove completely the template Cu(II), then washed with 0.1 mol L^{-1} sodium hydroxide solutions, and finally washed with deionized water till neutral pH and dried at 50℃. The obtained IIP/Al_2O_3 was sieved by 100 mesh size. Non-imprinted polymer/aluminum oxide (NIP/Al_2O_3) was also prepared with the same method but without the addition of Cu(II).

2.5. Adsorption experiments

2.5.1. Cu(II) adsorption studies

To study the adsorption of Cu(II) on IIP/Al_2O_3, the batch experiments were carried out under static

conditions. The Cu(II) concentrations in the supernatant solutions were determined by AAS. The stock solution for Cu(II) (1.0 g L^{-1}) was prepared by dissolving $CuSO_4{\cdot}5H_2O$ in deionized water.

The effect of pH on the adsorption capacity of IIP/Al_2O_3 was investigated in the pH range of from 2.0 to 5.5, at a temperature of 298 K, and at the Cu(II) concentration of 500 mg L^{-1}. The dosage of IIP/Al_2O_3 was kept constant at 0.5 g per 100 mL of solution. The pH values were adjusted by using the buffer solutions of sodium acetate/hydrochloric acid.

The effect of initial Cu(II) concentration on the adsorption capacity of IIP/Al_2O_3 was investigated at the Cu(II) concentration in the range of from 10 to 600 mg L^{-1}, at pH 5.0, and at a temperature of 298 K. The dosage of IIP/Al_2O_3 was also 0.5 g per 100 mL of solution.

Adsorption kinetics of Cu(II) on IIP/Al_2O_3 was performed by adding 0.25 g IIP/Al_2O_3 to 100 mL of Cu(II) solution (250 mg L^{-1}) at pH 5.0 with different contact times (1–60 min). Adsorption isotherm of Cu (II) on IIP/Al_2O_3 was performed by adding 0.5 g IIP/Al_2O_3 to 100 mL of Cu(II) solutions (10–500 mg L^{-1}) at pH 5 for 60 min. The adsorption kinetics and isotherm were studied at 298, 303, 308, and 313 K.

2.5.2. Selectivity studies

To investigate the selectivity of IIP/Al_2O_3 for Cu (II), the mixed solutions containing Cu(II), Zn(II), and Ni(II) were used. The volume of the mixed solution was 100 mL. The concentrations of Cu(II), Zn(II), and Ni(II) all were 250 mg L^{-1}. The dosage of IIP/Al_2O_3 or NIP/Al_2O_3 was 0.5 g. The selective adsorption was maintained for 60 min at 298 K. The concentrations of metal ions in the supernatant solutions were determined by AAS. The adsorption capacity, distribution ratio, selectivity factor, and relative selectivity factor were calculated by using the following equations:

$$Q_e = (C_0 - C_e)V/W \quad (1)$$

$$D = Q_e/C_e \quad (2)$$

$$\alpha = D_{Cu}/D_X \quad (3)$$

$$\alpha\prime = \alpha_{IP}/\alpha_{NP} \quad (4)$$

where Q_e is the adsorption capacity at equilibrium (mg g^{-1}); C_0 and C_e are the initial and equilibrium concentrations of the given metal ions (mg L^{-1}), respectively; V is the volume of metal ion solutions (mL); W is the mass of adsorbent (g); D is the distribution ratio (mL g^{-1}); α is the selectivity factor; D_{Cu} and D_X are the distribution ratios of Cu(II) and X (X = Ni(II) or Zn(II)), respectively; α' is the relative selectivity factor; and α_{IP} and α_{NP} are the selectivity factors of IIP/Al_2O_3 and NIP/Al_2O_3, respectively.

2.6. Desorption and reusability

In order to study the reusing possibility of IIP/Al_2O_3, a hydrochloric acid solution of 0.6 mol L^{-1} was used to desorb Cu(II) from the IIP/Al_2O_3. The adsorption capacity of IIP/Al_2O_3 for Cu(II) was determined in the process, and it was a important parameter to evaluate the stability of IIP/Al_2O_3.

3. Results and discussion

3.1. Characterization studies

3.1.1. FT-IR spectra

The FT-IR spectra of Al_2O_3, Al_2O_3 after silica deposit, CTS, IIP/Al_2O_3, and NIP/Al_2O_3 are shown in Fig. 2. The comparison of these IR spectra shows that IIP/Al_2O_3 and NIP/Al_2O_3 have a similar backbone. The FT-IR spectrum of the raw aluminum oxide powder shows two peaks at 1,634 and 958 cm^{-1} corresponding to the bending and asymmetric stretching vibration of Si–O, respectively (see Fig. 2, line a). After silica deposit and calcination, the peak at 943 cm^{-1} assigned to the stretching vibration of the Si–O increases significantly (see Fig. 2, line b), and this

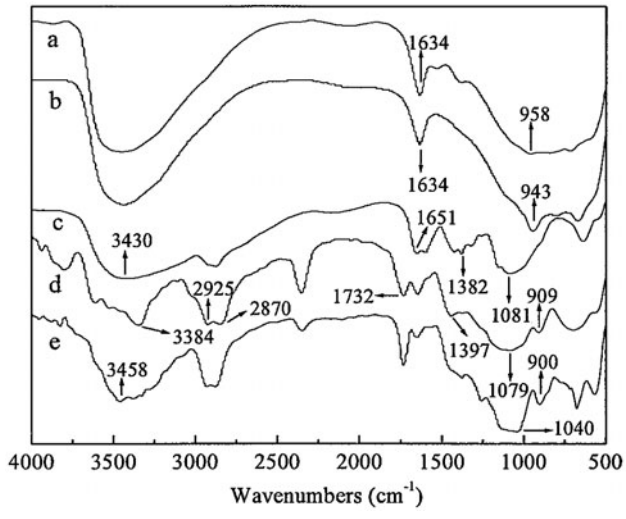

Fig. 2. FT-IR spectra of Al_2O_3 (a), Al_2O_3 after silica deposit (b), CTS (c), IIP/Al_2O_3 (d), and NIP/Al_2O_3 (e).

band is shifted to 909 cm^{-1} in IIP/Al_2O_3 [24] (see Fig. 2, line d). These results provide the evidence of an active SiO_2 layer formation and the introduction of reactive Si–O on the surface of aluminum oxide.

The band of C–O at 1,081 cm^{-1} in CTS (see Fig. 2, line c) is shifted to 1,079 cm^{-1} in IIP/Al_2O_3 (see Fig. 2, line d) and 1,040 cm^{-1} in NIP/Al_2O_3 (see Fig. 2, line e), respectively. A strong and overlapped band around 3,430 cm^{-1}, from stretching vibrations of N–H and O–H in CTS, is shifted to 3,384 cm^{-1} in IIP/Al_2O_3 and 3,458 cm^{-1} in NIP/Al_2O_3, respectively [12]. This indicates that the bands of N–H and O–H in the CTS involve in the coordination reaction with Cu(II). Moreover, δ_sN–H at 1,651 cm^{-1} and ν_{as} C–N at 1,382 cm^{-1} in CTS are shifted to 1,732 and 1,397 cm^{-1} in IIP/Al_2O_3, respectively. The spectrum of IIP/Al_2O_3 shows that the peaks of 2,925 and 2,870 cm^{-1}, from the stretching vibrations of C–H [19], enhance obviously in Fig. 2, line d. This is attributed to the $-CH_3$ group in IIP/Al_2O_3 derived from the crosslink agent KH-560. These results suggest that Cu(II) imprinted polymer has been grafted on the surface of Al_2O_3 after modification.

3.1.2. SEM and EDX analysis

The Al_2O_3, Al_2O_3 after silica deposit, IIP/Al_2O_3 and NIP/Al_2O_3 were characterized by using SEM in order to know the surface morphological images. As shown in Fig. 3(a), the raw Al_2O_3 particles have a serious reunion phenomenon. After silica deposit, the particles become more decentralized, and the surfaces of the particles are smoother (see Fig. 3(b)). There are obvious differences between the scanning electron micrographs of IIP/Al_2O_3 (see Fig. 3(c)) and NIP/Al_2O_3 (see Fig. 3(d)). The differences are probably due to the imprinting of Cu(II). Cu(II) was leached from the IIP/Al_2O_3, which would leave behind some cavities with the selectivity to Cu(II).

The EDX was used to analyze the elemental composition of Al_2O_3, Al_2O_3 after silica deposit, IIP/Al_2O_3, and NIP/Al_2O_3. The results are presented in Table 1. Compared with the raw Al_2O_3, silicon element increases significantly in Al_2O_3 after silica deposit. This is in accordance with the results of FT-IR spectra. In the IIP/Al_2O_3 and NIP/Al_2O_3, carbon and nitrogen elements appear, and their contents are higher than those of aluminum and silicon elements. This indicates that the ion-imprinted polymer is grafted onto the surface of Al_2O_3.

3.2. Adsorption of Cu(II)

3.2.1. Effects of pH and initial concentration on adsorption capacity at equilibrium

The effect of pH on Q_e was studied in the pH range of from 2.0 to 5.5. The results are shown in Fig. 4. Q_e increases rapidly with pH, and then reaches a maximum value. The observation may be explained as follows: Cu(II) and H^+ compete to form complexes with the active sites of the IIP/Al_2O_3. At a low pH, since there is the high concentration of H^+, more sites are occupied by H^+ at the expense of Cu(II). Thus, a

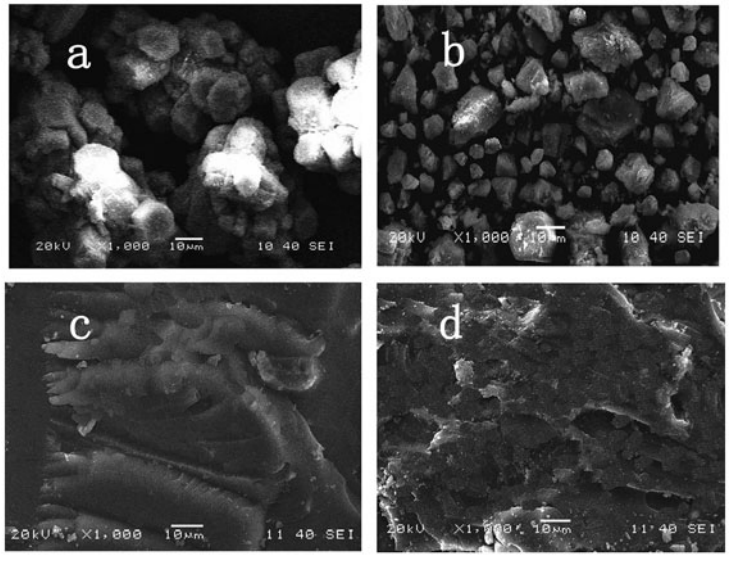

Fig. 3. SEM images of Al_2O_3 (a), Al_2O_3 after silica deposit (b), IIP/Al_2O_3 (c), and NIP/Al_2O_3 (d).

Table 1
Elemental compositions of Al_2O_3, Al_2O_3 after silica deposit, IIP/Al_2O_3, and NIP/Al_2O_3

Elements	Al_2O_3		Al_2O_3 after silica deposit		IIP/Al_2O_3		NIP/Al_2O_3	
	Mass (%)	Atom content (%)	Mass (%)	Atom content (%)	Mass (%)	Atom content (%)	Mass (%)	Atom content (%)
C	–	–	–	–	45.21	53.71	44.37	52.42
N	–	–	–	–	10.17	10.36	12.92	13.08
O	49.27	61.25	57.64	69.96	34.32	30.58	33.85	29.99
Al	49.52	37.89	25.81	18.56	2.700	1.480	0.7200	0.3900
Si	1.210	0.8600	16.55	11.48	7.600	3.870	8.140	4.120

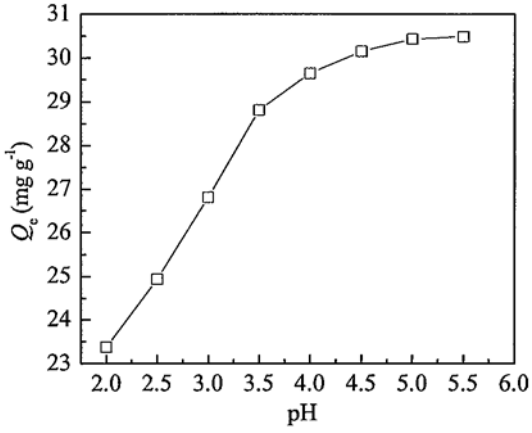

Fig. 4. Effect of pH on the adsorption capacity of Cu(II) on IIP/Al_2O_3 at equilibrium (initial concentration of Cu(II) = 500 mg L^{-1}; T = 298 K).

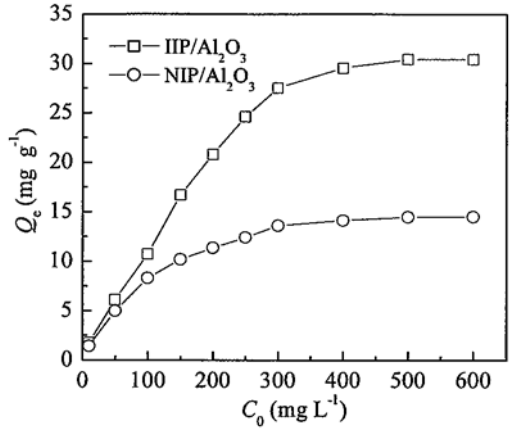

Fig. 5. Effect of initial concentration of Cu(II) on the adsorption capacity at equilibrium (pH 5.0; T = 298 K).

low Q_e value is obtained. At a higher pH, the new sites become available to be occupied by Cu(II), which results in the increase of Q_e. Singh and Mishra [25] reported similar results in the study on Cd(II) removal from aqueous solutions by using Cd(II) ion-imprinted polymer.

The effect of C_0 on Q_e was investigated at pH 5.0. The results obtained at C_0 between 10 and 600 mg L^{-1} are shown in Fig. 5. The Q_e values of IIP/Al_2O_3 and NIP/Al_2O_3 increase with C_0, and then do not change any more. It is obvious that the growth of Q_e for IIP/Al_2O_3 increases rapidly at the low C_0. Actually, when the initial concentration of Cu(II) is low, the IIP/Al_2O_3 can provide many active sites for the adsorption of Cu(II). After the C_0 reaches 300 mg L^{-1}, the growth of Q_e for IIP/Al_2O_3 increases slightly. This is due to the limited number of active sites with the increase of C_0. The maximum Q_e values of IIP/Al_2O_3 and NIP/Al_2O_3 are 30.42 and 11.49 mg/g, respectively. Compared with the Cu(II)-imprinted styrene-divinylbenzene beads [26], the Q_e value of IIP/Al_2O_3 is higher. The adsorption capacity of IIP/Al_2O_3 is larger than that of NIP/Al_2O_3, which indicates that the imprinting plays an important role in the adsorption process [27].

3.2.2. Adsorption kinetics

In order to study the adsorption kinetics of Cu(II) on IIP/Al_2O_3, the rate equations of Lagergren's pseudo-first-order (Eqs. (5) and (6)) and second-order (Eqs. (7) and (8)) were used to analyze the kinetic data.

$$dQ_t/dt = k_1(Q_e - Q_t) \quad (5)$$

$$\ln(Q_e - Q_t) = \ln Q_e - k_1 t \quad (6)$$

$$dQ_t/dt = k_2(Q_e - Q_t)^2 \quad (7)$$

$$t/Q_t = 1/(k_2 Q_e^2) + t/Q_e \quad (8)$$

where t is the adsorption time (min); Q_t and Q_e are the adsorption capacities at time t and equilibrium (mg g^{-1}), respectively; k_1 is pseudo-first-order rate constant (min^{-1}); and k_2 is pseudo-second-order rate constant (g mg^{-1} min^{-1}).

Fig. 6 shows the kinetic curves of adsorption of Cu(II) on IIP/Al_2O_3 at 298, 303, 308, and 313 K. It is cleanly seen that the adsorption rates increase rapidly at first 15 min, then increase slowly, and finally reach the equilibrium. Compared with other Cu(II) ion-imprinted polymer [16], the adsorption rate of Cu(II) on IIP/Al_2O_3 appears to be faster. Using Eq. (6), a ln(Q_e–Q_t) vs. t plot was prepared at different temperatures in which the data were fitted according to a line (not shown). The k_1 and Q_{ec} (theoretical adsorption capacity at equilibrium) were obtained from the slope and intercept of the plot, and given in Table 2. Using Eq. (8), the data were further analyzed by plotting t/Q_t vs. t (see Fig. 7). The k_2 and Q_{ec} were obtained from the plot. The results are also shown in Table 2. From Table 2, compared with the pseudo-first-order model, the correlation coefficients (R^2) of pseudo-second-order model are higher, and the Q_{ec} values of pseudo-second-order model are closer to the experimental Q_e values. Thus, the adsorption rate may be controlled by the chemical reaction mechanism through sharing or exchanging of electrons between Cu(II) and IIP/Al_2O_3 [28,29].

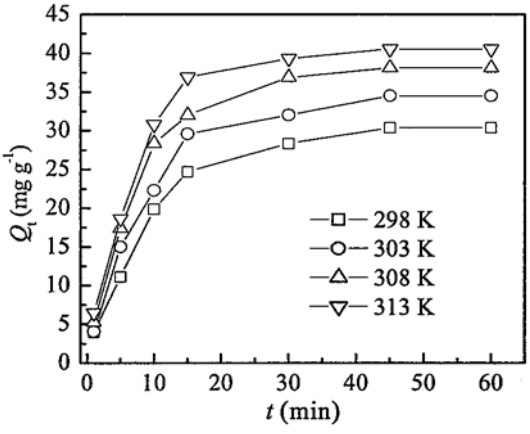

Fig. 6. Kinetic curves for the adsorption of Cu(II) on IIP/Al_2O_3 (initial concentration of Cu(II) = 250 mg L^{-1}; pH 5.0).

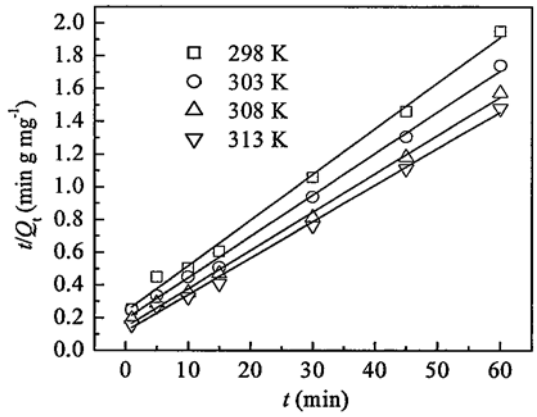

Fig. 7. Pseudo-second-order kinetics for the adsorption of Cu (II) on IIP/Al_2O_3 (initial concentration of Cu(II) = 250 mg L^{-1}; pH 5.0).

According to Arrhenius equation, the apparent activation energy can be calculated by using the Eq. (9).

$$\ln k_2 = -E_a/RT + \ln A \quad (9)$$

where E_a is the apparent activation energy (kJ mol^{-1}); R is the gas constant (8.314 J mol^{-1} K^{-1}); T is the absolute temperature (K); and A is the pre-exponential factor. An ln k_2 vs. $1/T$ plot was prepared in which the data were fitted according to a line, and shown in Fig. 8. A straight line was obtained with the correlation coefficient of 0.9938. E_a can be calculated from the slope of the plot, and is 15.7 kJ mol^{-1}.

Table 2
Comparison of pseudo-first-order and pseudo-second-order models for the adsorption of Cu(II) on IIP/Al_2O_3 (initial concentration of Cu(II) = 250 mg L^{-1}; pH 5.0)

T (K)	Q_e (mg g^{-1})	Pseudo-first order			Pseudo-second order		
		Q_{ec} (mg g^{-1})	k_1 (min^{-1})	R^2	Q_{ec} (mg g^{-1})	k_2 (g mg^{-1} min^{-1})	R^2
298	30.38	27.07	0.08423	0.9765	35.79	0.003253	0.9954
303	34.49	28.49	0.08802	0.9378	39.53	0.003401	0.9972
308	38.10	34.48	0.1132	0.9955	42.71	0.003914	0.9972
313	40.53	33.49	0.1182	0.9592	44.78	0.004348	0.9964

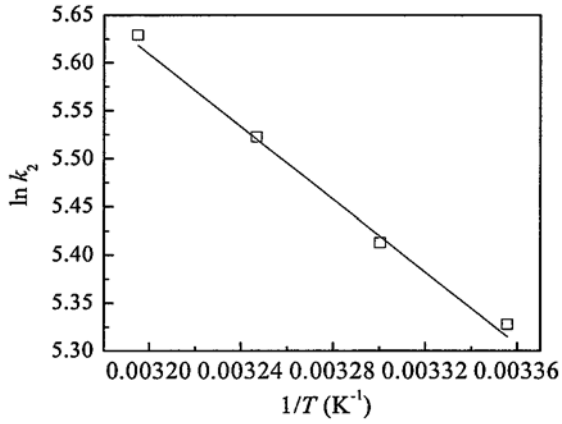

Fig. 8. The natural logarithm of adsorption rate constant as a function of the reciprocal of temperature (initial concentration of Cu(II) = 250 mg L^{-1}; pH 5.0).

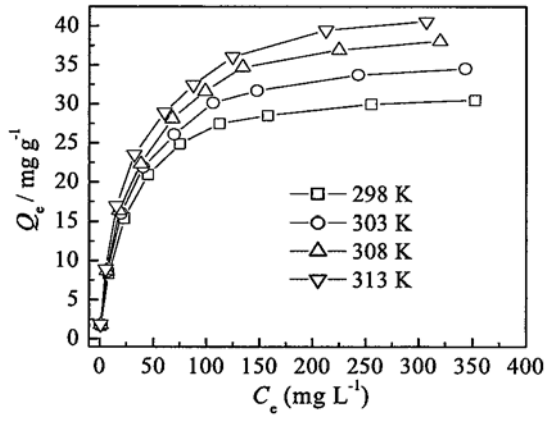

Fig. 9. Adsorption isotherms for Cu(II) on IIP/Al_2O_3 at 298, 303, 308, and 313 K (pH 5.0).

3.2.3. Adsorption isotherms

In order to study the adsorption isotherms of Cu (II) on IIP/Al_2O_3, the Langmuir (Eqs. (10) and (11)), Freundlich (Eqs. (12) and (13)), and Temkin (Eq. (14)) models were used to analyze the isotherm data.

$$Q_e = k_L Q_m C_e (1 + k_L C_e) \quad (10)$$

$$C_e/Q_e = C_e/Q_m + 1/(k_L Q_m) \quad (11)$$

$$Q_e = k_F C_e^{1/n} \quad (12)$$

$$\ln Q_e = \ln C_e/n + \ln k_F \quad (13)$$

$$Q_e = RT(\ln a_t + \ln C_e) b_t \quad (14)$$

where Q_e is the adsorption capacity at equilibrium (mg g^{-1}); Q_m is the maximal adsorption capacity (mg g^{-1}); C_e is the equilibrium concentration of Cu(II) (mg L^{-1}); k_L is the Langmuir constant; k_F and n are the Freundlich constants; and a_t and b_t are the Temkin constants.

Fig. 9 shows the adsorption isotherms for IIP/Al_2O_3 at 298, 303, 308, and 313 K. Q_e increases rapidly with C_e at first, then increases slowly, and finally almost does not vary. Using Eq. (11), the plot of C_e/Q_e vs. C_e is used to validate the Langmuir isotherm (see Fig. 10). Q_m and k_L are calculated from the slope and intercept of the plots, and given in Table 3. It can be seen that, the theoretical Q_m values (31.35 mg g^{-1} at 298 K, 34.66 mg g^{-1} at 303 K, 38.91 mg g^{-1} at 308 K, and 41.39 mg g^{-1} at 313 K) are close to the experimental Q_m values (30.47 mg g^{-1} at 298 K, 34.51 mg g^{-1} at 303 K, 38.03 mg g^{-1} at 308 K, and

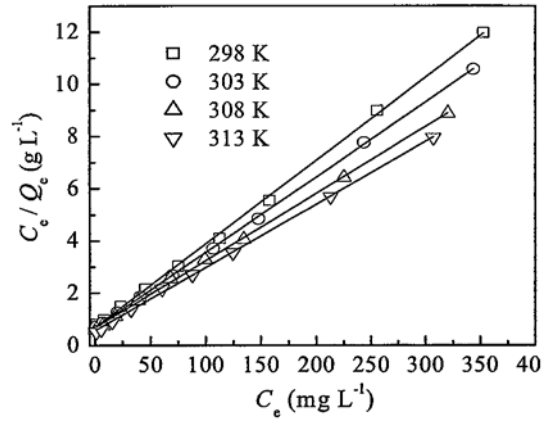

Fig. 10. Langmuir isotherms for the adsorption of Cu(II) on IIP/Al_2O_3 (pH 5.0).

40.59 mg g^{-1} at 313 K). Thus, the adsorption capacity increases with temperature. This may be due to the increase of temperature enhancing the accessibility of the active binding sites. Similar results have been obtained by Pan et al. [12] in the study of an ion-imprinted polymer based on palygorskite as a sacrificial support for selective removal of strontium(II). Using Eq. (13), an ln Q_e vs. ln C_e plot (not shown) is prepared to validate the Freundlich isotherm. The constant k_F and exponent n are obtained from the plot and also shown in Table 3. The results indicate that the values of n are close to 2 at different temperatures, so the IIP/Al_2O_3 can adsorb Cu(II) easily from the aqueous solutions. Using Eq. (14), the data are further analyzed with the linearized form of Temkin isotherm by plotting Q_e vs. ln C_e (not shown). The calculated Temkin constants and the corresponding correlation coefficients are also shown in Table 3. From Table 3, the values of the

Table 3
Isotherm parameters for the adsorption of Cu(II) on IIP/Al_2O_3 at pH 5.0

T (K)	Langmuir isotherm			Freundlich isotherm			Temkin isotherm		
	Q_m (mg g^{-1})	k_L (L mg^{-1})	R^2	n	k_F (mg g^{-1})	R^2	a_t	b_t	R^2
298	31.35	0.04600	0.9991	1.998	2.319	0.8945	0.8220	0.0023	0.9713
303	34.66	0.04330	0.9998	1.986	2.528	0.8992	0.8540	0.0024	0.9797
308	38.91	0.03840	0.9992	1.948	2.661	0.9209	0.8460	0.0026	0.9820
313	41.39	0.04330	0.9993	1.964	3.019	0.9154	0.9760	0.0027	0.9801

correlation coefficients for Langmuir model ($R^2 > 0.999$) are higher than those for Freundlich and Temkin models. Thus, the Langmuir model is more suitable for the experimental data of the adsorption of Cu(II) on IIP/Al_2O_3.

For predicting the favorability of an adsorption system, the essential characteristics of the Langmuir equation can be expressed in term of a dimensionless factor R_L, which is defined by the following equation [30]:

$$R_L = 1/(1 + C_m k_L) \quad (15)$$

where C_m is the highest initial concentration of adsorbate (mg L^{-1}). The R_L value indicates whether the type of the isotherm is favorable ($0 < R_L < 1$), unfavorable ($R_L > 1$), linear ($R_L = 1$), or irreversible ($R_L = 0$). The R_L values for the adsorption of Cu(II) on IIP/Al_2O_3 and NIP/Al_2O_3 are 0.0417 and 0.105 (298 K), respectively, indicating that the adsorption is a favorable process.

3.2.4. Adsorption thermodynamics

The thermodynamics for the adsorption of Cu(II) on IIP/Al_2O_3 was studied at a temperature in the range of from 298 to 313 K. Free energy change ΔG (kJ mol^{-1}), enthalpy change ΔH (kJ mol^{-1}), and entropy change ΔS (kJ mol^{-1} K^{-1}) can be calculated by using the following equations:

$$\Delta G = -RT \ln K \quad (16)$$

$$\Delta G = \Delta H - T\Delta S \quad (17)$$

$$\ln K = -\Delta H/RT + \Delta S/R \quad (18)$$

where K is the equilibrium constant ($K = Q_e/C_e$). Using Eq. (18), an ln K vs. $1/T$ plot was prepared in which the data were fitted according to a straight line, and shown in Fig. 11. The correlation coefficient of the straight line is 0.9936. The values of ΔH and ΔS were obtained from the slope and intercept of the straight line. ΔH was calculated to be 21.68 kJ mol^{-1}, which revealed that the adsorption process of Cu(II) on IIP/Al_2O_3 was endothermic. The calculated ΔS was 0.0862 kJ mol^{-1} K^{-1}. The positive value of ΔS means the increase of the randomness for the adsorption process. By using Eq. (17), ΔG was calculated to be −3.996 kJ mol^{-1} at 298 K, −4.426 kJ mol^{-1} at 303 K, −4.857 kJ mol^{-1} at 308 K, and −5.288 kJ mol^{-1} at 313 K, respectively, which indicated the feasibility of the adsorption process [31].

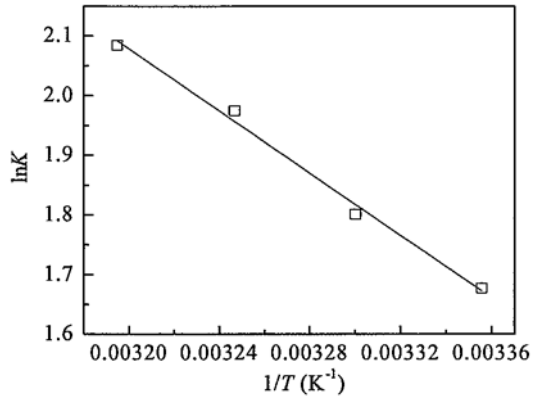

Fig. 11. The natural logarithm of equilibrium constant as a function of the reciprocal of temperature (pH 5.0).

3.3. Selectivity studies

The results of the adsorption rate for IIP/Al_2O_3 and NIP/Al_2O_3 are given in Fig. 12. IIP/Al_2O_3 shows higher adsorption rate of 71.5% for Cu(II), and lower adsorption rate of around 20% for Ni(II) and Zn(II). However, NIP/Al_2O_3 shows low adsorption rate for all metal ions. The D, α, and α' of Cu(II) with respect to Ni(II) and Zn(II) are summarized in Table 4. The α values of IIP/Al_2O_3 are higher than those of NIP/Al_2O_3. Due to the imprinting effect, IIP/Al_2O_3

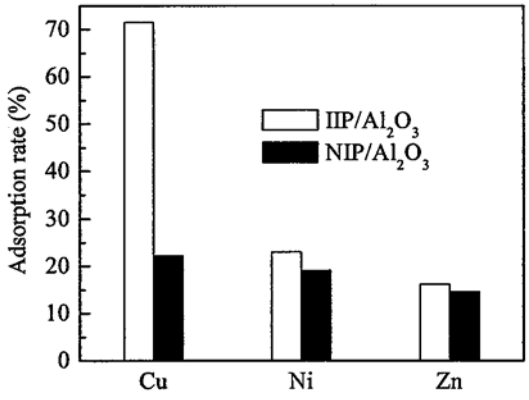

Fig. 12. Competitive adsorption of metal ions on IIP/Al_2O_3 and NIP/Al_2O_3 from the mixed solution containing Cu(II), Zn(II), and Ni(II) (pH 5.0; $T = 298$ K).

Table 4
The selectivity parameters of IIP/Al_2O_3 and NIP/Al_2O_3 (pH 5.0; $T = 298$ K)

	IIP/Al_2O_3		NIP/Al_2O_3		
Metal ions	D (mL g^{-1})	α	D (mL g^{-1})	α	α'
Cu(II)	501.8	–	57.40	–	–
Ni(II)	60.08	8.352	47.52	1.208	6.914
Zn(II)	38.66	12.98	34.19	1.679	7.731

yields the sites of special size for the selective recognition of Cu(II). The α' values of Cu(II)/Ni(II) and Cu (II)/Zn(II) are 6.914 and 7.731, respectively, indicating that the adsorption affinity of IIP/Al_2O_3 is about seven times larger than that of NIP/Al_2O_3. Compared with the Cu(II) ion-imprinted polymers reported in the literatures [16,32], the relative selectivity factors of Cu(II)/Ni(II) and Cu(II)/Zn(II) of IIP/Al_2O_3 are higher. Thus, IIP/Al_2O_3 has a specific selectivity to Cu (II), but non-specific selectivity to the other metal ions although these ions possess a similar chemical properties.

3.4. Reusability studies

The reusability of IIP/Al_2O_3 is likely to be a key factor in industrial application to improve economic benefits. After the Cu(II) adsorption-desorption cycles were repeated 10 times by using the same IIP/Al_2O_3 under the same experimental conditions, the adsorption capacity of IIP/Al_2O_3 is decreased only 2%. This reveals that IIP/Al_2O_3 shows good stability and reusable properties in the studied experimental conditions.

4. Conclusions

A new composite material of copper(II) ion-imprinted polymer/aluminum oxide was prepared successfully for selective adsorption of Cu(II) by grafting Cu(II)-imprinted polymer onto the surface of aluminum oxide. The IIP/Al_2O_3 shows good characteristics, such as high adsorption capacity, fast adsorption kinetics, high selectivity, and good reusability. The kinetics and mechanism for the adsorption of Cu(II) on the IIP/Al_2O_3 follow the Lagergren pseudo-second-order model and the Langmuir adsorption isotherm, respectively. In addition, the thermodynamics studies show the adsorption of Cu(II) on the IIP/Al_2O_3 is an endothermic and spontaneous process, indicating that the adsorption is controlled by the chemical reaction mechanism. The results demonstrate that the IIP/Al_2O_3 has a potential application for the selective removal/recovery of Cu(II) in aqueous solutions containing Cu(II).

Acknowledgments

This research is supported by the Hunan Provincial Natural Science Foundation of China (No. 13JJ3086). Also, the authors acknowledge the financial supports from a Project Supported by the National Natural Science Foundation of China (No. 20976040).

References

[1] H. Tapiero, D.M. Townsend, K.D. Tew, Trace elements in human physiology and pathology. Copper, Biomed. Pharmacother. 57 (2003) 386–398.
[2] H. Lee, J. Yi, Removal of copper ions using functionalized mesoporous silica in aqueous solution, Sep. Sci. Technol. 36 (2001) 2433–2448.
[3] S.H. Jo, S.Y. Lee, K.M. Park, S.C. Yi, D. Kim, S. Mun, Continuous separation of copper ions from a mixture of heavy metal ions using a three-zone carousel process packed with metal ion-imprinted polymer, J. Chromatogr. A 1217 (2010) 7100–7108.
[4] R. Say, E. Birlik, A. Ersöz, F. Yılmaz, T. Gedikbey, A. Denizli, Preconcentration of copper on ion-selective imprinted polymer microbeads, Anal. Chim. Acta 480 (2003) 251–258.
[5] D. Feng, C. Aldrich, H. Tan, Treatment of acid mine water by use of heavy metal precipitation and ion exchange, Miner. Eng. 13 (2000) 623–642.
[6] A.D. Dwivedi, S.P. Dubey, K. Gopal, M. Sillanpää, Strengthening adsorptive amelioration: Isotherm modeling in liquid phase surface complexation of Pb(II) and Cd (II) ions, Desalination 267 (2011) 25–33.

[7] D. Zhang, J.D. Crawford, R.A. Bartsch, Solvent extraction of divalent metal ions by lipophilic di-ionizable acyclic polyethers: Effect of end group variation, J. Incl. Phenom. Macro. Chem. 70 (2011) 205–216.
[8] G. Arthanareeswaran, V.M. Starov, Effect of solvents on performance of polyethersulfone ultrafiltration membranes: Investigation of metal ion separations, Desalination 267 (2011) 57–63.
[9] H.A. Maturana, I.M. Perič, B.L. Rivas, S.A. Amalia Pooley, Interaction of heavy metal ions with an ion exchange resin obtained from a natural polyelectrolyte, Polym. Bull. 67 (2011) 669–676.
[10] S. Oh, T. Kang, H. Kim, J. Moon, S. Hong, J. Yi, Preparation of novel ceramic membranes modified by mesoporous silica with 3-aminopropyltriethoxysilane (APTES) and its application to Cu^{2+} separation in the aqueous phase, J. Membr. Sci. 301 (2007) 118–125.
[11] E. Birlik, A. Ersöz, A. Denizli, R. Say, Preconcentration of copper using double-imprinted polymer via solid phase extraction, Anal. Chim. Acta 565 (2006) 145–151.
[12] J. Pan, X. Zou, Y. Yan, X. Wang, W. Guan, J. Han, X. Wu, An ion-imprinted polymer based on palygorskite as a sacrificial support for selective removal of strontium(II), Appl. Clay Sci. 50 (2010) 260–265.
[13] Buhani, Suharso, Sumadi, Adsorption kinetics and isotherm of Cd(II) ion on *Nannochloropsis* sp biomass imprinted ionic polymer, Desalination 259(1–3) (2010) 140–146.
[14] B. Godlewska-Żyłkiewicz, B. Leśniewska, I. Wawreniuk, Assessment of ion imprinted polymers based on Pd(II) chelate complexes for preconcentration and FAAS determination of palladium, Talanta 83 (2010) 596–604.
[15] D.K. Singh, S. Mishra, Synthesis and characterization of Hg(II)-ion-imprinted polymer: Kinetic and isotherm studies, Desalination 257 (2010) 177–183.
[16] D.K. Singh, S. Mishra, Synthesis of a new Cu(II) ion imprinted polymer for solid phase extraction and preconcentration of Cu(II), Chromatographia 70 (2009) 11–12.
[17] M. Khajeh, Z.S. Heidari, E. Sanchooli, Synthesis, characterization and removal of lead from water samples using lead-ion imprinted polymer, Chem. Eng. J. 166 (2011) 1158–1163.
[18] E. Birlik, A. Ersöz, E. Açıkkalp, A. Denizli, R. Say, Cr(III)-imprinted polymeric beads: Sorption and preconcentration studies, J. Hazard. Mater. 140 (2007) 110–116.
[19] C. Lin, H. Wang, Y. Wang, Z. Cheng, Selective solid-phase extraction of trace thorium(IV) using surface-grafted Th(IV)-imprinted polymers with pyrazole derivative, Talanta 81 (2010) 30–36.
[20] H. Su, J. Li, T. Tan, Adsorption mechanism for imprinted ion (Ni^{2+}) of the surface molecular imprinting adsorbent (SMIA), Biochem. Eng. J. 39 (2008) 503–509.
[21] C. Li, J. Gao, J. Pan, Z. Zhang, Y. Yan, Synthesis, characterization, and adsorption performance of Pb(II)-imprinted polymer in nano-TiO_2 matrix, J. Environ. Sci. 21 (2009) 1722–1729.
[22] M. Shamsipur, J. Fasihi, K. Ashtari, Grafting of ion-imprinted polymers on the surface of silica gel Particles through covalently surface-bound initiators: A selective sorbent for uranyl ion, Anal. Chem. 79 (2007) 7116–7123.
[23] Y. Li, B. Gao, R. Du, Studies on preparation and recognition characteristic of surface-ion imprinting material IIP-PEI/SiO_2 of chromate anion, Sep. Sci. Technol. 46 (2011) 1472–1481.
[24] X. Zhu, X. Chang, Y. Cui, X. Zou, D. Yang, Z. Hu, Solid-phase extraction of trace Cu(II) Fe(III) and Zn(II) with silica gel modified with curcumin from biological and natural water samples by ICP-OES, Microchem. J. 86 (2007) 189–194.
[25] D.K. Singh, S. Mishra, Synthesis, characterization and removal of Cd(II) using Cd(II)-ion imprinted polymer, J. Hazard. Mater. 164 (2009) 1547–1551.
[26] A. Tobiasz, S. Walas, B. Trzewik, P. Grzybek, M.M. Zaitz, M. Gawin, H. Mrowiec, Cu(II)-imprinted styrene–divinylbenzene beads as a new sorbent for flow injection-flame atomic absorption determination of copper, Microchem. J. 93 (2009) 87–92.
[27] I. Dakova, I. Karadjova, I. Ivanov, V. Georgieva, B. Evtimova, G. Georgiev, Solid phase selective separation and preconcentration of Cu(II) by Cu(II)-imprinted polymethacrylic microbeads, Anal. Chim. Acta 584 (2007) 196–203.
[28] A.R. Iftikhar, H.N. Bhatti, M.A. Hanif, R. Nadeem, Kinetic and thermodynamic aspects of Cu(II) and Cr (III) removal from aqueous solutions using rose waste biomass, J. Hazard. Mater. 161 (2009) 941–947.
[29] Y. Zhai, Y. Liu, X. Chang, X. Ruan, J. Liu, Metal ion-small molecule complex imprinted polymer membranes: Preparation and separation characteristics, React. Funct. Polym. 68 (2008) 284–291.
[30] W. Guo, W. Hu, J. Pan, H. Zhou, W. Guan, X. Wang, J. Dai, L. Xu, Selective adsorption and separation of BPA from aqueous solution using novel molecularly imprinted polymers based on kaolinite/Fe_3O_4 composites, Chem. Eng. J. 171 (2011) 603–611.
[31] S.S. Gupta, K.G. Bhattacharyya, Adsorption of Ni(II) on clays, J. Colloid Interface Sci. 295 (2006) 21–32.
[32] S. Walas, A. Tobiasz, M. Gawin, B. Trzewik, M. Strojny, H. Mrowiec, Application of a metal ion-imprinted polymer based on salen–Cu complex to flow injection preconcentration and FAAS determination of copper, Talanta 76 (2008) 96–101.